Ecosystem Health and Sustainability
A SCIENCE PARTNER JOURNAL

RESEARCH ARTICLE

Integrating Landscape Ecological Risk and Ecosystem Services for Ecological Zoning in the Qilian Mountain National Park

Juchuan Gao, Ninghui Pan*, and Dongmei Zhou*

College of Resources and Environmental Sciences, Gansu Agricultural University, Lanzhou 730070, China.

*Address correspondence to: pannh@gsau.edu.cn (N.P.); zhoudm@gsau.edu.cn (D.Z.)

Citation: Gao J, Pan N, Zhou D. Integrating Landscape Ecological Risk and Ecosystem Services for Ecological Zoning in the Qilian Mountain National Park. *Ecosyst. Health Sustain.* 2025;11:Article 0441. https://doi.org/10.34133/ehs.0441

Submitted 19 June 2025
Revised 24 September 2025
Accepted 22 October 2025
Published 21 November 2025

Qilian Mountain National Park, serving as a vital ecological barrier in northwest China, urgently requires achieving a balance between conservation and management. This study aims to elucidate the spatiotemporal dynamics of landscape patterns, landscape ecological risks (LERs), and ecosystem services (ESs), and reveal their response relationships. Based on risk-service response optimization, ecological zoning is established, and adaptive strategies are proposed. The research integrates multi-source data within a "pattern–process–service–sustainability" framework, employing methods including landscape indices, the multiscale geographically weighted regression (MGWR) model, the LER-ES coupling model, and the Geodetector model. Key findings are as follows: (a) Landscape fragmentation decreased by 12.3% from 2000 to 2020, with an average annual reduction of 2.1% in LER and weakened spatial clustering intensity. An east–west gradient in LER persisted. (b) The comprehensive capacity of ESs improved, exhibiting a southeast–northwest gradient distribution. (c) The MGWR model confirmed that LER negatively impacts ecological services, with spatial nonstationarity present. (d) Ecological zones were classified into protected areas, stable areas, sensitive areas, and vulnerable areas, with obvious differences in driving factors—environmental vulnerability was primarily dominated by natural factors, while relatively stable areas were more significantly influenced by human activities. This represents the first zoning based on the risk-service relationship, breaking through traditional limitations.

Introduction

Under the combined pressures of global climate change and intensified human activity, global ecosystems are experiencing unprecedented levels of disturbance vulnerability [1,2]. Such disturbances, by altering the spatial configuration of landscape patterns such as fragmentation and reduced connectivity [3], further drive the degradation of ecosystem functions, shifts in ecosystem types, and imbalances in critical ecological processes like material cycling and energy flows [4]. Mountain ecosystems, as quintessential fragile ecological zones, exhibit amplified cascade effects due to their complex topographic conditions and heightened climate sensitivity, driving threshold-exceeding ecological perturbations, most notably accelerated pedogenesis disruption and defaunation cascades [5]. This not only threatens regional ecological security but also undermines ecosystem service (ES) functions like water conservation and soil retention, ultimately compromising human welfare and socioecological system sustainability [6]. The contemporary "pattern–process–service–sustainability"" paradigm in landscape ecology accordingly presents an integrated lens for analyzing ecological hierarchies, facilitating comprehensive characterization of regional ecosystem architecture processes, and service characteristics, clarifying their intrinsic linkages, and scientifically managing ecosystems to achieve regional sustainable development [7].

Landscape pattern change serves as both a direct indicator of ecosystem evolution and a spatial reflection of the dynamic interplay between anthropogenic activities and natural processes [8,9]. With the intensification of planetary-scale climate perturbations and land-use expansion, accelerated urbanization has led to significant alterations in landscape patterns, such as forest fragmentation, agricultural expansion, and wetland shrinkage [3,10]. These regime shifts compromise fundamental biogeochemical processes essential for biodiversity conservation and carbon sequestration while attenuating key provisioning and regulating services (soil moisture retention, slope stability, and atmospheric regulation), generating cascading risks for regional sustainable development pathways. Therefore, identifying regional landscape ecological risks (LERs) based on a clear understanding of landscape patterns helps elucidate the response mechanisms of regional ecosystems while correspondingly generating theoretical foundations for sustainable land-use allocation and ecological network design, and managing sustainable development [11].

ESs represent the cornerstone of anthropogenic life-support systems and socioeconomic progress, with their sustainable supply governed by the cascading relationships within the "landscape pattern–ecological process–service function" framework [12]. Rapid landscape changes significantly influence the formation and delivery of ESs by altering key ecological processes including energy flows, material cycles, and species migration [13]. From a compositional perspective, shifts in land-use proportions directly affect essential ESs. For example, every 10% reduction in forest coverage may lead to a 15% to 20% decline in watershed water conservation capacity [14]. In terms of spatial configuration, enhanced landscape connectivity can facilitate species migration and gene flow, thereby improving biodiversity maintenance services. Existing studies have demonstrated that when the landscape fragmentation index exceeds 0.25, pollination service efficiency decreases significantly [15]. The destabilization within this "landscape–ecological function–wellbeing" coupling poses systemic risks, simultaneously endangering environmental security and human development trajectories through the deterioration of pivotal services including soil fertility maintenance, precipitation recycling, and greenhouse gas balancing. Therefore, building upon the quantification of key regional ESs, further elucidation of the interactions between LERs and ESs will help to optimize regional landscape patterns and key ecological processes., ultimately promoting sustainable socioecological development in the region [16].

Confronting intersecting global environmental threats and nation-state development objectives, the scientific governance of natural resources and the harmonization of ecological protection with economic development have emerged as critical priorities for the international community. Consequently, ecological functional zoning has emerged and gradually developed into a crucial research direction at the intersection of ecology, geography, and environmental management [17]. Within this context, the integration of LER assessment with ES evaluation has emerged as a foundational framework for ecological functional zoning methodologies [18]. By integrating the interactive mechanisms of "risk-service", it provides a scientific basis for regional sustainable development. Domestic and international studies indicate that traditional zoning often focuses on single-factor assessments, whereas a coupled framework can more systematically reveal the spatial correlation between ecosystem vulnerability and service provision capacity under human-induced pressures. Using spatially explicit analytics to decode landscape-driven risk trajectories and their service function implications (e.g., the antagonistic relationship between water conservation and soil erosion risk), key conflict areas can be identified, enabling relatively precise zoning and regulation strategies [19]. Simultaneously, diagnosing the dominant factors driving spatial heterogeneity in zoning coupling outcomes helps elucidate ecological differentiation mechanisms, offering targeted guidance for regional territorial spatial planning and ecological restoration projects, as well as informing tailored management measures to enhance ecosystem resilience under the "dual carbon" goals.

As a flagship member of China's first cohort of 10 national parks, Qilian Mountain National Park shoulders the fundamental mandate of "prioritizing ecological conservation". The integrity of its ESs is paramount for safeguarding regional ecological security. Nevertheless, facing synergistic pressures from climatic system alterations and human-driven ecosystem perturbations, the park confronts multifaceted ecological challenges including (a) accelerated glacier retreat and consequent water resource stress, (b) progressive degradation of grassland ecosystems, (c) permafrost thaw-induced hydrological regime shifts, and (d) precipitous biodiversity loss. Within the national park's tripartite zoning framework (core conservation zone, ecological restoration zone, and traditional use zone), there exists a pressing need to develop a theoretically robust zoning system rooted in landscape ecology principles. This system should facilitate the holistic protection of the park's integrated "mountain–river–forest–farmland–lake–grassland–desert" integrated system. Addressing this imperative, our study adopts an innovative "landscape pattern–ecological process–ecosystem service" coupling framework to (a) establish a scientifically validated ecological functional zoning system for Qilian Mountain National Park and (b) identify key drivers of risk-service heterogeneity across zones to inform differentiated conservation strategies that balance ecological integrity with socioeconomic development. Notably, compared with existing studies, this research marks the first attempt to conduct ecological functional zoning by examining the response relationship between LERs and ES functions. While advancing this innovation, it further refines the overall research framework—strengthening its theoretical rigor and practical applicability—and initially explores the framework's universality. This exploration is intended to lay the groundwork for its future promotion and application in ecological functional zoning for other national parks within China's national park network. To operationalize this innovative and refined framework, the specific research objectives are to (a) quantify the spatiotemporal dynamics of landscape configuration (2000–2020) and develop an integrated ecological vulnerability metric to assess risk trajectory, (b) assess spatiotemporal heterogeneity in the provision of critical ESs across decadal scales (2000–2020), (c) unravel the coupled dynamics between landscape-mediated risk regimes and ES delivery, and (d) develop a coupled risk-service zoning framework, identify dominant heterogeneity factors, and formulate zone-specific management protocols. The study's outcomes will enhance the ecological security framework and resilience of Qilian Mountain National Park, provide evidence-based support for conservation policy formulation, and establish a transferable paradigm for ecological functional zoning in China's expanding national park network. By bridging theoretical innovation with practical management needs, this research holds substantial value for advancing China's national park governance system and achieving ecological civilization goals.

Materials and Methods

Overview of the study area

Qilian Mountain National Park (94°10′E to 103°04′E, 36°43′N to 39°19′ N) occupies a pivotal ecotone in northwestern China, straddling the Qinghai–Gansu provincial border at the triple junction of the Tibetan Plateau, Inner Mongolia Plateau, and Loess Plateau geomorphic domains. Functioning as a pivotal ecological safeguard and climatic modulator in China's arid northwest region, the region has an average elevation exceeding 3,800 m and covers a total area of 50,200 km^2. It harbors diverse ecosystems, including glaciers, alpine meadows, forests, and deserts, exhibiting pronounced landscape heterogeneity (Fig. 1).

Climatically, the area features a typical continental plateau climate, characterized by low annual temperatures and precipitation regimes averaging 400 mm $year^{-1}$. The vegetation is highly diverse, encompassing alpine meadows, coniferous forests, and shrublands, which is the most important habitat for rare animals such as snow leopard, Tibetan antelope, and white-lipped deer. The region exhibits exceptionally high ecological sensitivity. In recent years, climate system alteration and anthropogenic factors have triggered localized grassland degradation,

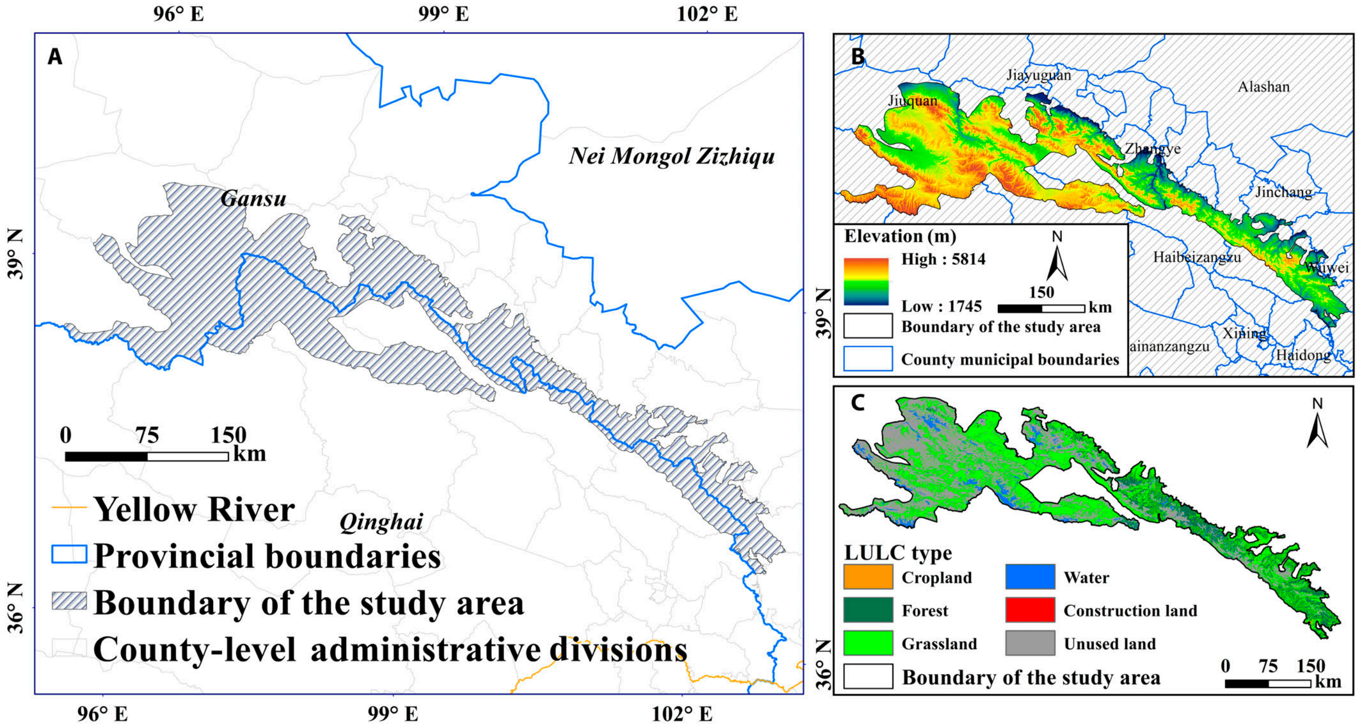

Fig. 1. Map of Qilian Mountain National Park. (A) Geographical location. (B) Elevation. (C) Land use/cover (LULC) type.

reduced forest coverage, and diminished landscape connectivity. Key ecological processes—such as glacier meltwater recharge, soil erosion, and species migration—interact dynamically with landscape patterns, further influencing the delivery of ESs. These challenges pose significant threats to regional sustainable development.

Technical framework

The technical framework is shown in Fig. 2.

Data sources

The research utilized multiple datasets obtained from various sources, which were systematically processed to meet the study's objectives [20–23]. The original data information and sources are listed in Table 1.

Methods

Landscape pattern indices and LER assessment

Landscape pattern metrics serve as effective tools to distill complex landscape composition information into quantifiable indices, enabling accurate monitoring and characterization of regional landscape composition and spatial configuration [24,25]. To systematically quantify the landscape structure of Qilian Mountain National Park, we employed 9 carefully selected landscape metrics that capture both compositional and configurational characteristics. For detailed information, please refer to Supplementary Material 2.

LER denotes the probability of adverse impacts on ecosystem integrity and biodiversity resulting from alterations in landscape spatial configuration [26]. In this study, we implemented the landscape ecological risk index (LERI) methodology to evaluate ecological risks across Qilian Mountain National Park. The LERI was computed through an integrated assessment framework combining landscape loss indices, derived from both landscape disturbance and vulnerability indices:

$$LERI_i = \sum_{i=1}^{n} \frac{A_{ki}}{A_k} \times R_i \tag{1}$$

where $LERI_i$ represents the landscape ecological risk index, A_{ki} denotes the area of the ith landscape type within the kth evaluation unit, A_k is the total area of all landscape types in the kth evaluation unit, n is the total number of landscape types, and R_i serves as the LERI for the kth evaluation unit. The magnitude of R_i determines the degree of LER, with a higher value indicating greater risk.

This study systematically assessed the LER dynamics of Qilian Mountain National Park in 2000, 2010, and 2020 via a spatially explicit risk evaluation framework. Its results were spatially visualized with ArcGIS 10.5 and classified into 5 risk levels (lower: 0 to 0.2; low: 0.2 to 0.4; medium: 0.4 to 0.6; high: 0.6 to 0.8; higher) using the equal interval classification method.

ES assessment

The integrated valuation of ecosystem services and tradeoffs (InVEST) model is a spatially explicit analytical framework by Stanford University's Natural Capital Project, used to quantify and map ES flows under alternative management scenarios [27]. This study quantitatively assessed 4 critical ESs in Qilian Mountain National Park using the InVEST model. All required data for the assessment are provided in Supplementary Material 3.

Based on the ecological function positioning, environmental degradation characteristics, conservation needs, and research objectives of Qilian Mountain National Park, this study selects 4 key ESs—habitat quality, carbon storage, water yield, and soil conservation—for assessment.

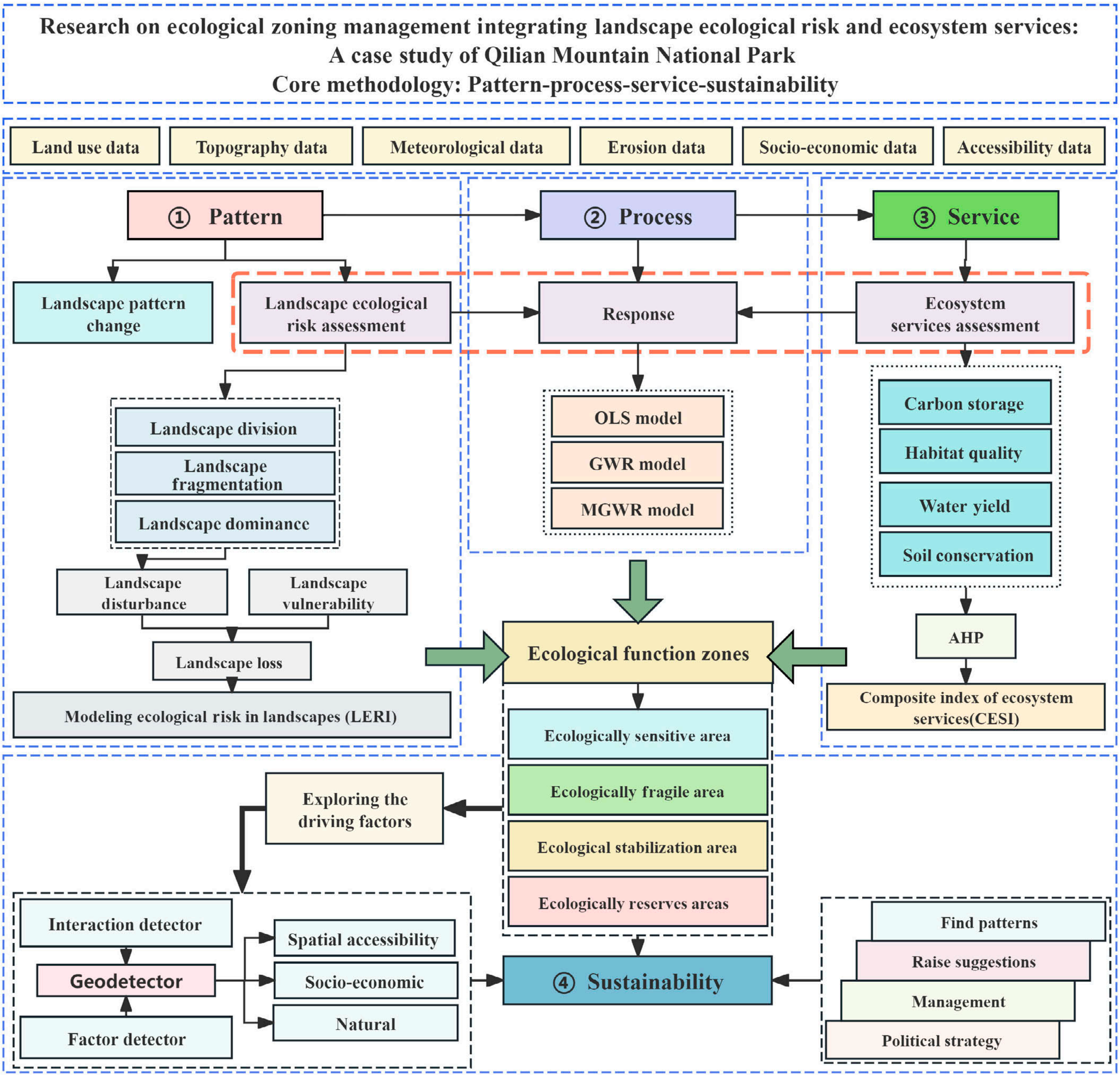

Fig. 2. Technical framework.

Among them, habitat quality responds to the demand for the park to serve as a "biodiversity conservation area", enabling the reflection of how ecological degradation and human activities affect habitats and supporting the optimization of biodiversity conservation strategies. Carbon storage is associated with the mountainous area's function of "carbon sequestration and oxygen release", which allows the evaluation of the climate regulation benefits of ecological degradation and conservation projects, as well as filling the research gap in the carbon cycle of alpine ecosystems. Water yield aligns with the park's positioning as a "core water conservation area", which can reflect the impact of degradation such as glacier retreat on water supply functions and quantify the improvement effect of relevant conservation projects on freshwater provision. Soil conservation addresses the worsening issue of soil erosion, reflects the ecosystem's erosion resistance capacity, and lays the foundation for analyzing the trade-off/synergy relationships among services.

Habitat quality

The habitat quality module within the InVEST model is a spatially explicit tool designed to assess ecosystem habitat conditions and quantify their vulnerability to anthropogenic threats [28,29].

$$Q_{zj} = H_j\left(1 - \left(\frac{D_{zj}^z}{D_{zj}^z + k^z}\right)\right) \tag{2}$$

Table 1. Data sources.

Type	Name	Format	Resolution	Source
Land Use data	Land use/cover (LULC)	Tiff	30 m	Resource and Environmental Science Data Platform (https://www.resdc.cn)
Topography data	DEM	Tiff	30 m	Geospatial data cloud (https://www.gscloud.cn)
	Slope	Tiff	30 m	Geospatial data cloud (https://www.gscloud.cn)
Meteorological data	Average annual temperature	Tiff	1 km	National Tibetan Plateau / Third Pole Environment Data Center (http://data.tpdc.ac.cn).
	Average annual precipitation	Tiff	1 km	National Tibetan Plateau / Third Pole Environment Data Center (http://data.tpdc.ac.cn).
	evapotranspiration	Tiff	1 km	National Tibetan Plateau / Third Pole Environment Data Center (http://data.tpdc.ac.cn).
Erosion data	Rainfall erosion	Tiff	1 km	Geographic Data Sharing Infrastructure, global resources data cloud (www.gis5g.com)
	Soil erosion	Tiff	1 km	Geographic Data Sharing Infrastructure, global resources data cloud (www.gis5g.com)
Vegetation data	Root Restricting Layer Depth	Tiff	250 m	ISRIC Soil Data Hub (https://data.isric.org/)
	Plant Available Water Content	Tiff	1 km	National Tibetan Plateau / Third Pole Environment Data Center (http://data.tpdc.ac.cn).
	Net Primary Productivity (NPP)	Tiff	500 m	In National Glacial Permafrost Desert Science Data (http://www.ncdc.ac.cn)
Socio-economic data	GDP	Tiff	1 km	Resource and Environmental Science Data Platform (https://www.resdc.cn)
	POP	Tiff	1 km	Resource and Environmental Science Data Platform (https://www.resdc.cn)
Accessibility data	Highway	Shp.	-	Open Street Map (https://osm.mapplus.cn)
	Watershed	Shp.	-	Open Street Map (https://osm.mapplus.cn)

$$D_{xj}=\sum_{r=1}^{R}\sum_{y=1}^{Y_r}\left(\frac{\omega_r}{\sum_{r=1}^{R}\omega_r}\right)r_y i_{rzy}\beta_x S_{jr} \quad (3)$$

where Q_{xj} denotes the habitat quality of raster x in land-use type j; H_j denotes the habitat suitability of land-use type J; D_{xj} denotes the level of stress to which raster x in land-use type j is subjected; Z denotes the normalization constant; K denotes the scaling constant. r denotes the number of coercion factors; r is a coercion factor; y is the number of rasters of coercion factor r; Y_r is the number of rasters accounted for by the coercion factor; ω_r is the stressor weight, value range 0 to 1; i_{rxy} is the effect of stressor r on the raster of the habitat; β_x is the level of habitat resistance to disturbance; and S_{jr} is the relative sensitivity of different habitats to each stressor.

Carbon storage

Carbon storage is key for ecosystem carbon potential; quantifying it aids assessing climate impacts and carbon neutrality [30].

$$C_{total}=C_{above}+C_{below}+C_{soil}+C_{dead} \quad (4)$$

where C_{total} denotes total carbon, C_{above} denotes aboveground biomass carbon (e.g., trees and shrubs), C_{below} denotes belowground biomass carbon (roots), C_{soil} denotes soil organic carbon (0 to 30 cm depth), and C_{dead} denotes litter carbon.

Water yield

The InVEST model assesses regional water yield spatially via ecosystem parameters [31]. Z is an empirical parameter, several subwatersheds were selected in the study area and different values were set to simulate the water yield of each watershed in comparison with the measured values of average runoff, and it was found that the fit was higher when the value was equal to 2.78.

$$\mathrm{Z}=(\omega-1.25)\mathrm{P}/\mathrm{AWC} \quad (5)$$

where P and AWC are average values of precipitation and available water capacity, respectively, in the study area. AWC is the volumetric (mm) plant available water content.

$$Y(x) = \left(1 - \frac{AET(x)}{P(x)}\right)P(x) \tag{6}$$

where $Y(x)$ is the annual water yield (mm) of pixel grid x, $AET(x)$ is the annual actual evapotranspiration (mm) of pixel grid x, and $P(x)$ is the annual rainfall (mm) of pixel grid x.

Soil conservation

The InVEST model's sediment delivery ratio (SDR) module uses a spatially distributed method to quantify soil retention capacity. It first generates watershed spatial distribution data from elevation data and then calculates sediment yield for each grid cell. Soil conservation capacity is calculated as the difference between potential soil erosion and actual soil erosion [32].

$$A_m = RKLSCP \tag{7}$$

$$A_p = RKLS \tag{8}$$

$$A_c = A_m - A_p \tag{9}$$

where A_a denotes actual soil erosion (t ha^{-1} year^{-1}), A_a represents potential soil erosion (t ha^{-1} year^{-1}), Ac (t ha^{-1} year^{-1}) is the soil conservation capacity, R is the rainfall erosivity factor, K is soil erodibility, L denotes slope length, S denotes steepness, C reflects vegetation cover and management practices, and P accounts for erosion control measures.

Composite index of ESs

The composite ecosystem services index (CESI) is derived by standardizing, normalizing, and weighting the 4 ESs described above [33,34].

$$ES_i = \frac{S_i - S_{i,min}}{S_{i,max} - S_{i,min}} \tag{10}$$

S_i is the original value of the ith ES. $S_{i,min}$ and $S_{i,max}$ are the minimum and maximum values of the ith ES in the study area, respectively. ES_i is the standardized value of the ith ES.

The analytic hierarchy process is employed to determine the weight W_i for each ES. Calculation results are included in Supplementary Materials 3, Table S6.

$$CESI = \sum_{i=1}^{n} \left(ES_i \times W_i\right) \tag{11}$$

$CESI$ denotes the ES composite index, n is the number of types of ESs, and W_i denotes the weight of ES type i.

Linear regression model

OLS model

Ordinary least squares (OLS) is a classical linear regression method used to estimate the linear relationship between a dependent variable and one or more independent variables [35].

$$y_i = \beta_0 + \sum_{k=1}^{p} \beta_k x_{ik} + \epsilon_i \tag{12}$$

where y_i denotes the predicted variable, x_{ik} is the independent variable, β_0 denotes the intercept, β_k is the regression coefficient, and ϵ_i denotes the random error.

GWR model

Geographically weighted regression (GWR) extends traditional regression by allowing parameter estimates to vary across geographic space, capturing spatial nonstationarity in relationships between dependent and independent variables [36].

$$y_i = \beta_0\left(U_i, V_i\right) + \sum_{k=1}^{p} \beta_k\left(U_i, V_i\right)x_{ik} + \epsilon_i \tag{13}$$

where (U_i, V_i) denotes spatial coordinates of location I and β_k (U_i, V_i) denotes the local regression coefficient of the kth independent variable at location I. The rest of the parameters are the same as for the OLS model.

MGWR model

Multiscale geographically weighted regression (MGWR) advances traditional GWR model by allowing for variable-specific bandwidth; it allows for different explanatory variables to be run at different spatial scales, thus capturing spatial heterogeneity more flexibly [37].

$$y_i = \beta_0\left(U_i, V_i\right) + \sum_{k=1}^{p} \beta_k\left(U_i, V_i | b_k\right)x_{ik} + \epsilon_i \tag{14}$$

where β_k (U_i, $v_i | b_k$) is the regression coefficient of the kth variable at location (U_i, V_i) with bandwidth b_k. The rest of the parameters are the same as for the OLS model.

Ecological function zones

The 4-quadrant method is a classification approach based on dual-indicator cross-analysis. By employing the LERI and comprehensive ecosystem service index as the x axis and y axis, respectively, this method constructs a 2-dimensional spatial matrix to divide the study area into 4 functional zones.

Specifically, the first quadrant is an area with important ES functions and high LER, such as important river water sources. These areas have key service functions but are susceptible to disturbance and difficult to restore once damaged. The second quadrant is an area with unimportant ESs but high LER. These areas are mainly unused, with a small proportion of service functions but fragile ecosystems. The third quadrant includes areas with low ecological service importance and low LER, such as heavily modified areas with frequent human activity, where ecological services are weak but resilient to disturbance. The fourth quadrant comprises areas with important ecological services but low sensitivity, such as large-scale forests, which have strong disturbance resistance and the ability to self-regulate and recover. Through this framework, the ecological characteristics of different areas within the park can be systematically and comprehensively understood, providing a robust foundation for developing targeted, scientifically sound ecological conservation and management strategies.

In this study, we first standardized the calculated 2020 LERI and CESI values, using their medians (0.386 and 0.462, respectively) as threshold boundaries to establish an ecological functional zoning Cartesian coordinate system. Based on their combined positions within this coordinate system, Qilian Mountain National Park was classified into 4 distinct ecological zones. The primary partitions are based on the criteria we have listed in Supplementary Material 4, Table S7.

Spatial heterogeneity

Global spatial autocorrelation

Global spatial autocorrelation quantifies the degree of nonrandom spatial patterning exhibited by georeferenced variables throughout a defined geographical extent. The degree of spatial clustering is typically quantified using Moran's I index [38].

$$I = \frac{n}{\sum_{i=1}^{n} \left(x_i - \overline{x}\right)^2} \frac{\sum_{i=1}^{n} \sum_{j=1}^{n} \left(x_i - \overline{x}\right)\left(\left(x_j - \overline{x}\right)\right)}{\sum_{i=1}^{n} \sum_{j=1}^{n} W_{ij}} \quad (15)$$

where n is the total number of evaluation units; x_i and x_j denote the values of the results of the ith and jth evaluation units, respectively; $\overline{x}$ is the average value of the evaluation results; and W_{ij} is the adjacency weight between the ith and jth evaluation units.

Local spatial autocorrelation

Local spatial autocorrelation is often assessed via the LISA (local indicators of spatial association) framework, which quantifies the spatial dependency between geographic features and their values. Analyzing the LISA statistic enables identification of significant spatial clustering—including high-concentration zones (hot spots) and low-concentration zones (cold spots)—and their precise locations [39].

$$I_i = \left(x_i - \overline{x}\right) \frac{\sum_{i=1}^{i} W_{ij}\left(x_j - \overline{x}\right)}{\frac{1}{n} \sum_{j=1}^{n} \left(x_i - \overline{x}\right)^2} \quad (16)$$

where the significance of each indicator is the same as the global spatial autocorrelation

Driver exploration

The Geodetector method effectively captures spatial homogeneity within regions and heterogeneity between regions, thereby revealing the spatial differentiation patterns of research subjects [40]. This model operates on the principle that if (X) exerts a substantial influence on (Y), their respective spatial distributions should demonstrate statistically significant covariation. This approach not only identifies spatial stratification heterogeneity of geographical phenomena but also determines the dominant driving factors behind such heterogeneity while quantitatively assessing interaction effects between factors. For detailed information, please refer to Supplementary Material 5.

$$q = 1 - \frac{\sum_{h=1}^{L} N_h \sigma_h^2}{N\sigma^2} \quad (17)$$

where q denotes the spatial decentralized explanatory power, Nh denotes the number of samples at stratum h, ${\sigma_h}^2$ is the variance of the dependent variable Y within the hth stratum, N denotes the total number of samples, and σ^2 is the variance of the global dependent variable Y.

The identification of driving factors is critical for exploring the mechanisms of ecological zoning. Based on a systematic review of domestic and international literature and the unique ecosystem characteristics of Qilian Mountain National Park, this study classified driving factors into 3 categories via a multidimensional, systematic approach. Natural factors include DEM (digital elevation model), slope, net primary productivity (NPP), average annual precipitation, and average annual temperature, collectively characterizing the region's topographic features and hydrothermal conditions. Socioeconomic factors are represented by population density and gross domestic product (GDP) to quantify human activity intensity. Spatial accessibility factors include distance to water systems and roads, acting as effective indicators of potential anthropogenic disturbances to ecosystems.

All driving factors were spatially visualized via GIS (geographic information system) technology, laying a solid data foundation for subsequent quantitative analysis. This comprehensive driving factor framework not only follows universal principles in landscape ecology research but also integrates the study area's region-specific considerations.

Results

Landscape pattern change and LER assessment

Changes in landscape pattern indices assessment

The results demonstrate significant differences in 9 landscape pattern indices among these land cover types, along with distinct dynamic trends over time (Fig. 3).

Analyzing the landscape composition and quantitative characteristics, the landscape composition of the study area showed obvious stratification: Grassland, as the dominant type, maintained the highest percentage of landscape all year round and, together with unused land and forest, constituted the regional landscape matrix. The results of patch density and the number of patches show that grassland has the characteristic of foundational fragmentation, while the number of built-up land patches is the lowest, with only 126 patches, but the patch density [PD (patch density) = 0.0025] reveals that its spatial distribution is highly concentrated. From 2000 to 2020, the percentage of landscape of water (W) increased by 77.1%, reflecting a significant expansion of its area.

The study of landscape morphology and stability characteristics can be found, the edge density of grassland and unused land is the highest, at 17.87 and 13.2, respectively, and the boundary interaction is active, while the landscape division of construction land is 15.63, which is far more than other types, confirming its extreme fragmentation. Meanwhile, grassland had a low degree of landscape division despite the high number of patches. Landscape dominance metrics reflect the dominance of landscape types in the landscape pattern. Grassland and unused land have a high degree of dominance; forest also has a degree of dominance. Analyzing the landscape disturbance and landscape loss, the construction land has both a high degree of disturbance and a high degree of loss, and its ecological vulnerability is outstanding; in contrast, the stability indexes of the grassland and the forest indicate that they are more resistant to disturbance.

The spatiotemporal changes of LERs

Temporal variation analysis

From 2000 to 2020, the LER of Qilian Mountain National Park showed a distinct temporal pattern of "initial improvement followed by stabilization" (Fig. 4). Regionally, medium-risk areas dominated the risk profile, accounting for over 50% in all 3 study periods, while higher-risk areas accounted for the least (less than 0.5% in each period). During 2000–2010, the spatial extent of high-risk zones contracted markedly from 10,869.22 to 6,832.98, a decrease of 37.2%, accompanied by significant spatial reorganization: Higher-risk areas shrank by 12.1%, medium-risk areas expanded by 16.1%, and low-risk and lower-risk areas increased

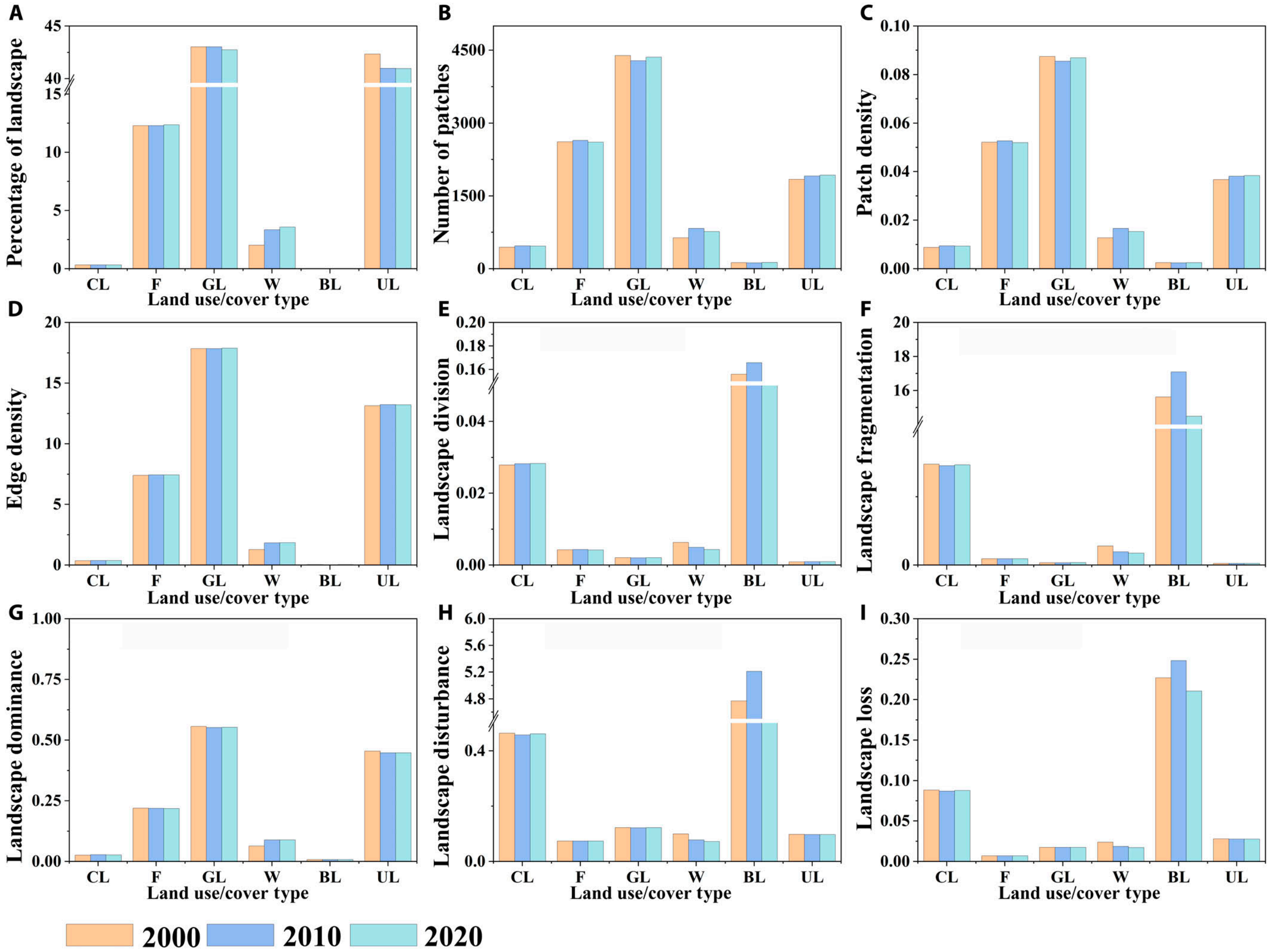

Fig. 3. Mapping the change in Qilian Mountain National Park pattern index, 2000–2020. CL, cropland; F, forest; GL, grassland; W, water; BL, construction land; UL, unused land. (A) Proportion of different land use/land cover types within the landscape. (B) Total number of patches for a specific land use/land cover type. (C) Number of patches per unit area for a given land use/land cover type. (D) Measures the total length of landscape patch edges per unit area. (E) Quantifies the degree of landscape fragmentation, with higher values indicating greater fragmentation. (F) Landscape fragmentation, reflecting the degree of landscape division; higher values signify more severe fragmentation. (G) Landscape dominance, reflecting the extent to which a particular land use/cover type prevails within the landscape. (H) Degree of landscape disturbance, indicating the impact of human activities or natural factors on the landscape. (I) Measures landscape loss, reflecting the extent of landscape degradation or disappearance.

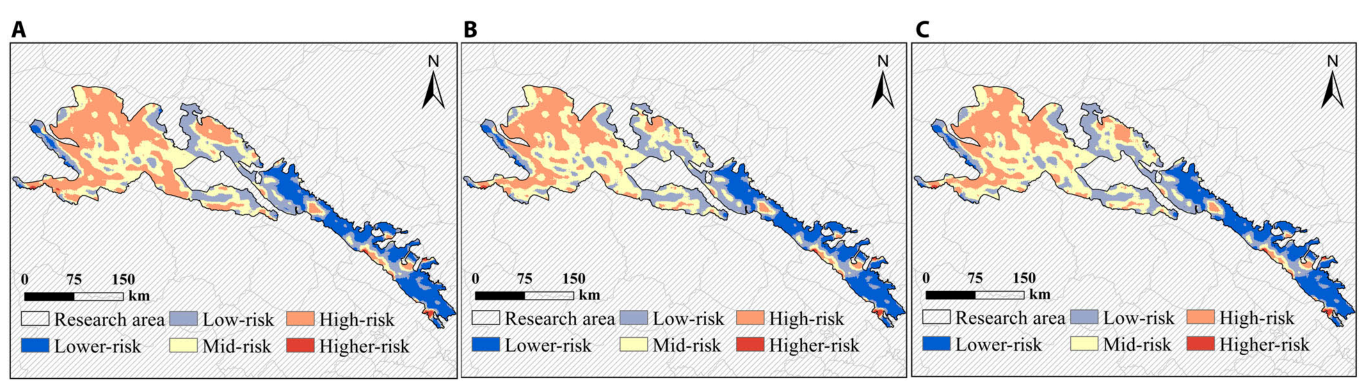

Fig. 4. Spatial distribution of LERs. (A) 2000. (B) 2010. (C) 2020.

modestly by 1.4% and 7.1%, respectively. Nearly 40% (4,330.34 km^2) of the baseline high-risk territory transitioned to medium-risk, and the global Moran's I index decreased from 0.589 to 0.563, indicating the spatial disaggregation of western high-risk clusters and enhanced overall ecosystem security. After 2010, the risk landscape reached relative equilibrium with only localized fluctuations: High-risk zones continued to decline slightly by approximately 3.4%, while the other 4 risk zones remained

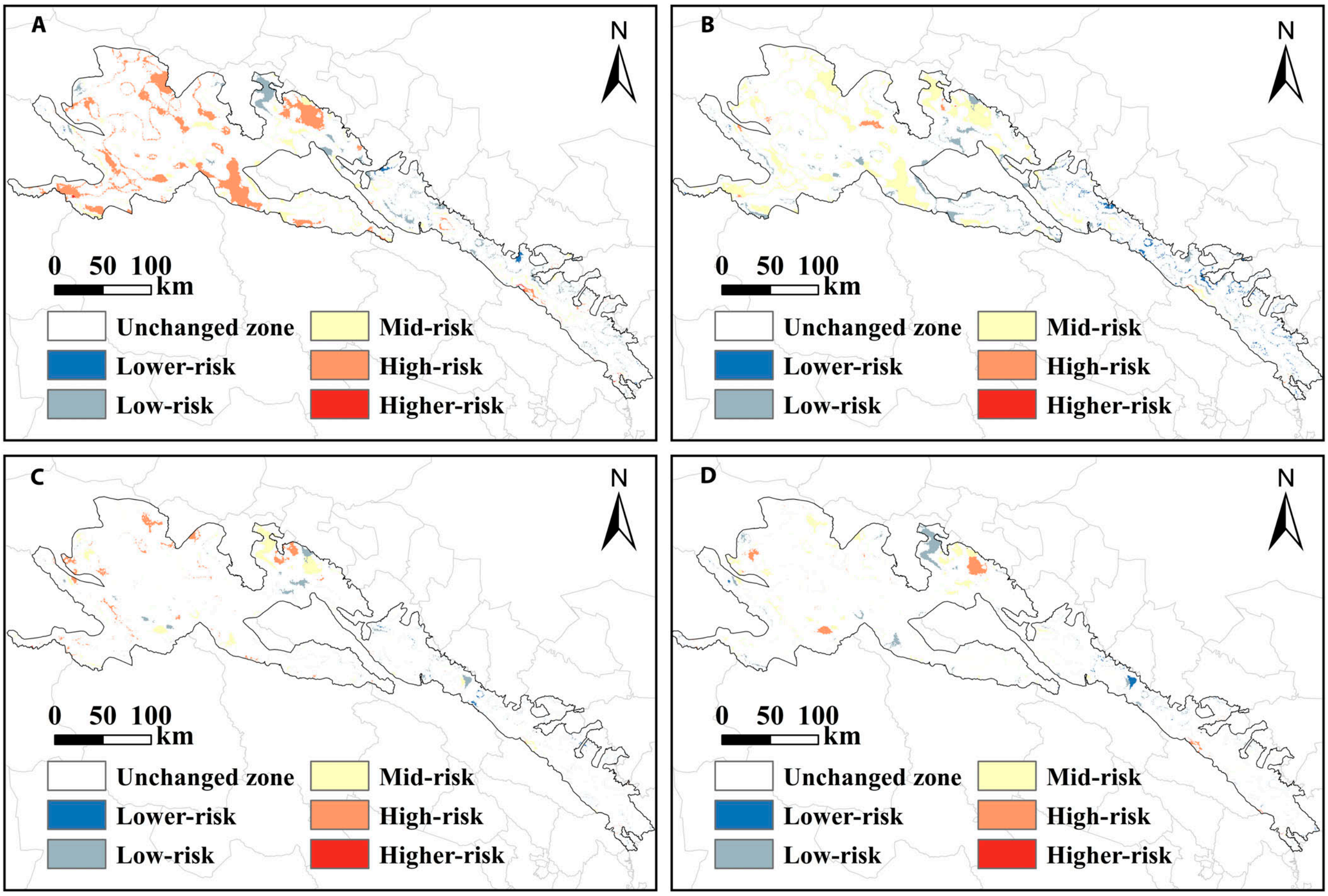

Fig. 5. LER changes from 2000 to 2020. (A) 2000–2010 transfer out. (B) 2000–2010 shift to. (C) 2010–2020 transfer out. (D) 2010–2020 shift to.

basically stable. The main risk transition was from medium-risk to low-risk (670.23 km^2, accounting for 4.3% of 2010's medium-risk areas) (Fig. 5). Throughout the 20-year period, the global Moran's I indices (2000: 0.589; 2010: 0.563; 2020: 0.577) consistently showed statistically significant positive spatial autocorrelation.

Spatial variation analysis

Spatially, the LER of Qilian Mountain National Park exhibited a pronounced longitudinal gradient, with risk levels decreasing progressively from west to east. Higher-risk and high-risk zones (high-value areas) were predominantly concentrated in the western sector and scattered across the entire region; medium-risk zones mainly occupied the western and west–central regions; and lower-risk zones were primarily concentrated in the eastern sector. Western areas accounted for most ecological risk transformations, showing a consistent de-escalation from high to low risk (Fig. 4). Local spatial autocorrelation analysis revealed that LER was regionally clustered, mainly in "high–high" (H–H) and "low–low" (L–L) patterns: In 2000, the western sector was the core aggregation zone for H–H clusters (corresponding strongly to high-risk zones), while the eastern sector was the core for L–L clusters (core low-risk areas), with sporadic outlier units ("high–low" and "low–high" clusters). By 2020, the spatial pattern had adjusted: H–H agglomerations became further fragmented, with western high-value agglomerations distributed in a point-like manner; L–L agglomerations showed increased stability, with clearer boundaries of eastern low-value agglomerations; and outliers across the study area decreased, with fewer patches in "H–L" and "L–H" agglomerations than in 2010, leading to a significant reduction in spatial heterogeneity (Supplementary Material 1, Fig. S1).

Spatiotemporal characteristics of ES evolution

Temporal analysis revealed consistent improvement in habitat quality across Qilian National Park from 2000 to 2020, with mean values increasing from 0.4332 to 0.4469. The spatial configuration exhibited a distinct southeast–northwest gradient, with superior habitat conditions predominantly located in southeastern sectors (Fig. 6A to C). Total carbon sequestration capacity demonstrated a significant positive trend (0.00068 $year^{-1}$), increasing from 0.4332 to 0.4469 between 2000 and 2020 (Fig. 6D to F).

The study area exhibited significant increases in water yield over the 2000–2020 period, with depth measurements rising from 635.86 mm to 654.59 mm. Total water yield showed a net increase of 0.22×10^8 m^3, peaking at 5.21×10^8 m^3 in 2010 before stabilizing at 4.41×10^8 m^3 in 2020. Spatially, the distribution of water production was heterogeneous, and the distribution pattern was stable during the study period (Fig. 6G to I). Soil erosion has changed drastically, with soil erosion per unit of watershed decreasing from 104.123 tons to 35.21 tons, and the area of drastic soil erosion in 2000 was mainly located in the eastern section of the Qilian Mountain National Park, and by 2010, soil erosion had been significantly reduced, with

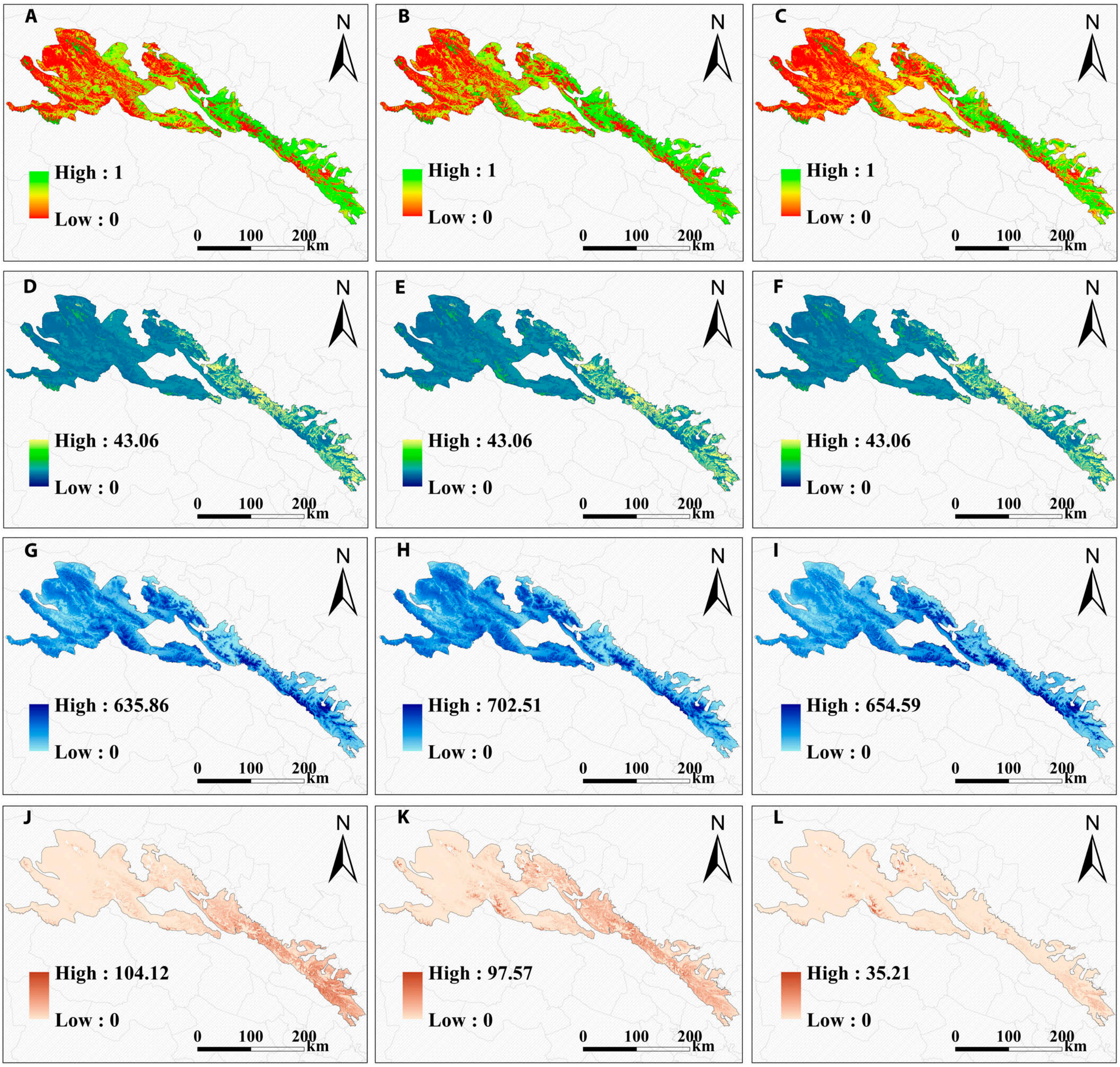

Fig. 6. ES assessment from 2000 to 2020. (A to C) Habitat quality in 2000, 2010, and 2020. (D to F) Carbon storage in 2000, 2010, and 2020. (G to I) Water yield in 2000, 2010, and 2020. (J to L) Soil conservation in 2000, 2010, and 2020.

soil erosion in the entire study area decreasing dramatically by 2020 (Fig. 6J to L).

Linking ESs and LER

Selection of regression methods

The combination of OLS regression ($R^2 = 0.68$, $P < 0.01$) and VIF (variance inflation factor) verification (mean = 4.2 ± 1.8) demonstrated both significant ES-LERI relationships and statistically orthogonal predictors, meeting all assumptions for valid linear modeling (Supplementary Material 6, Table S9).

The spatial distribution of R^2 showed strong heterogeneity across the study area, with areas of strong explanatory power for habitat quality concentrated in the southeast and areas of weak explanatory power dominated in the central and western parts of the country. The explanatory power of carbon sequestration was high, with high values concentrated in the northern and southern foothills of the Qilian Mountains. GWR revealed distinct spatial patterns in explanatory power: Water yield showed stronger influence in western regions (dominated by unused land and grassland ecosystems), while soil conservation exhibited greater explanatory power in eastern areas (characterized by construction land and cropland cover)

Three complementary regression approaches were employed to characterize the relationships between LER and 4 key ESs, enabling both global and localized analysis of these associations. The performance of each model was evaluated and compared based on AICc (Akaike information criterion corrected)

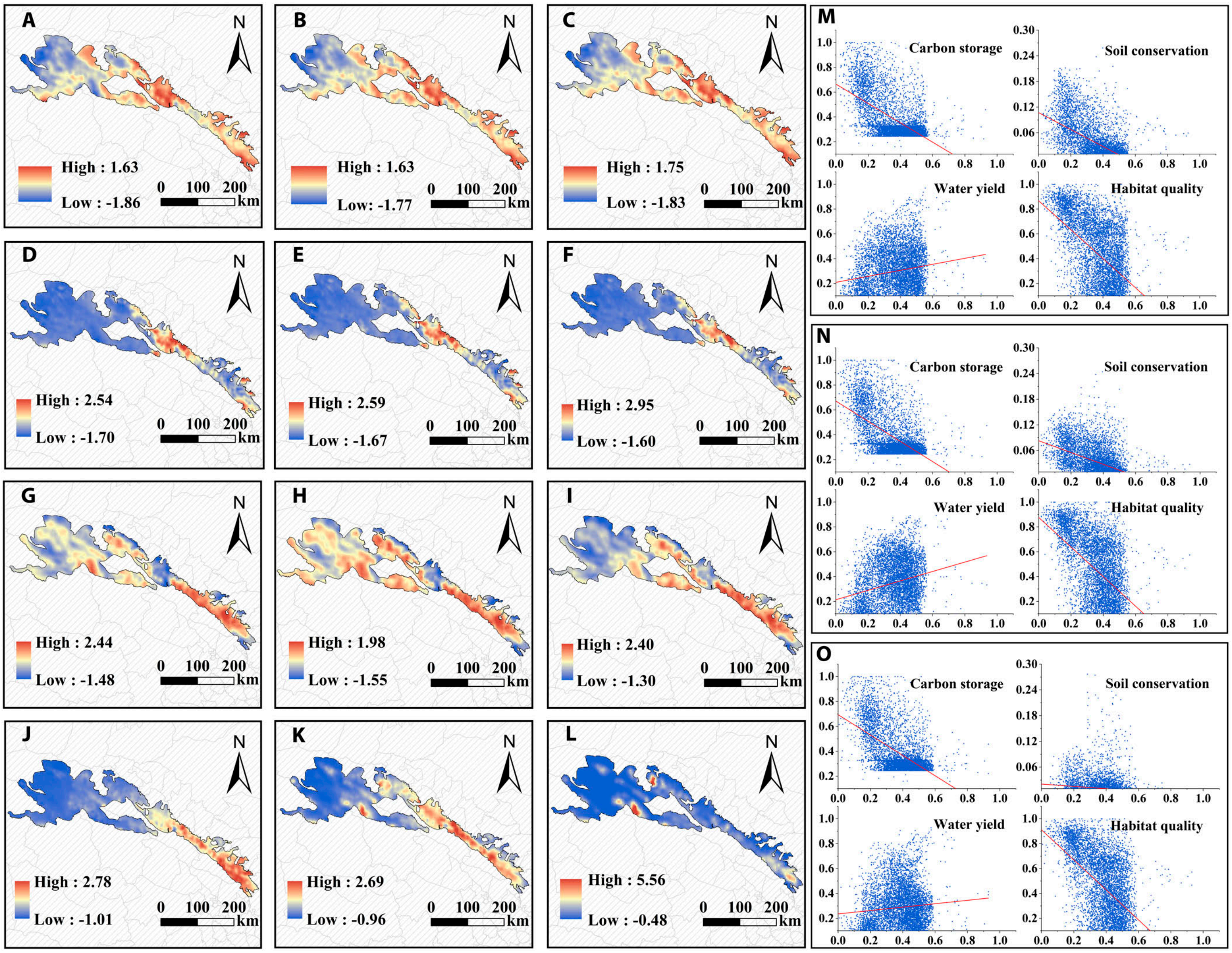

Fig. 7. Spatial distribution of MGWR model regression coefficients. (A to C) Habitat quality in 2000, 2010, and 2020. (D to F) Carbon storage in 2000, 2010, and 2020. (G to I) Water yield in 2000, 2010, and 2020. (J to L) Soil conservation in 2000, 2010, and 2020. (M to O) Scatterplot of regression coefficients in 2000, 2010, and 2020.

and R^2 values, where a lower AICC indicates poorer model fit and a higher R^2 represents better fitting performance. The MGWR approach substantially outperformed conventional models, achieving superior goodness-of-fit (R^2 = 0.82) while simultaneously capturing scale-dependent relationships between ecological risk and ESs (Supplementary Material 6, Table S10).

Coupling analysis of LER and ESs

Regression coefficients reveal significant spatial patterns in risk effect intensity across the study area (Fig. 7). LERs exert predominantly positive effects on habitat quality. Conversely, areas with negative coefficients show a declining trend (Fig. 7A to C). The spatial coverage of negative impacts on carbon storage significantly exceeds that of positive effects. During the study period, the maximum positive regression coefficient increased from 2.54 to 2.95, while the minimum negative coefficient rose from −1.70 to −1.60 (Fig. 7D to F). The intensity of LER's impact on soil sequestration significantly strengthened over the 2 decades. The maximum coefficient jumped from 2.78 to 5.56, while the minimum coefficient improved from −1.01 to −0.48 (Fig. 7J to L).

Ecological functional zones

In 2020, Qilian Mountain National Park exhibited a distinct southeast–northwest dichotomy, with LER and composite ESs demonstrating inverse spatial patterns (Fig. 8A and B). This antagonistic relationship informed our ecological functional zoning using a 4-quadrant analytical framework (Fig. 8D), revealing critical trade-offs between risk exposure and service provision.

Research indicates that natural forests dominate ecologically reserves areas, forming a structurally intact and functionally stable ecosystem network. Ecologically stable areas exhibit a discrete distribution pattern, primarily located in the peripheral zones of protected areas. Serving as critical transitional buffer zones between protected areas and sensitive regions, these areas are characterized by forest, grassland, and aquatic ecosystems, exhibiting typical "low-service, low-risk" attributes. Ecologically sensitive areas are concentrated in the central region of Qilian Mountain National Park, exhibiting pronounced "high-service, high-risk" characteristics. While possessing robust ES provisioning capacity, these zones simultaneously endure significant LER pressures. Ecologically fragile areas are primarily situated in the park's northwest, dominated by grasslands and idle lands with relatively simple ecosystem structures. These zones endure

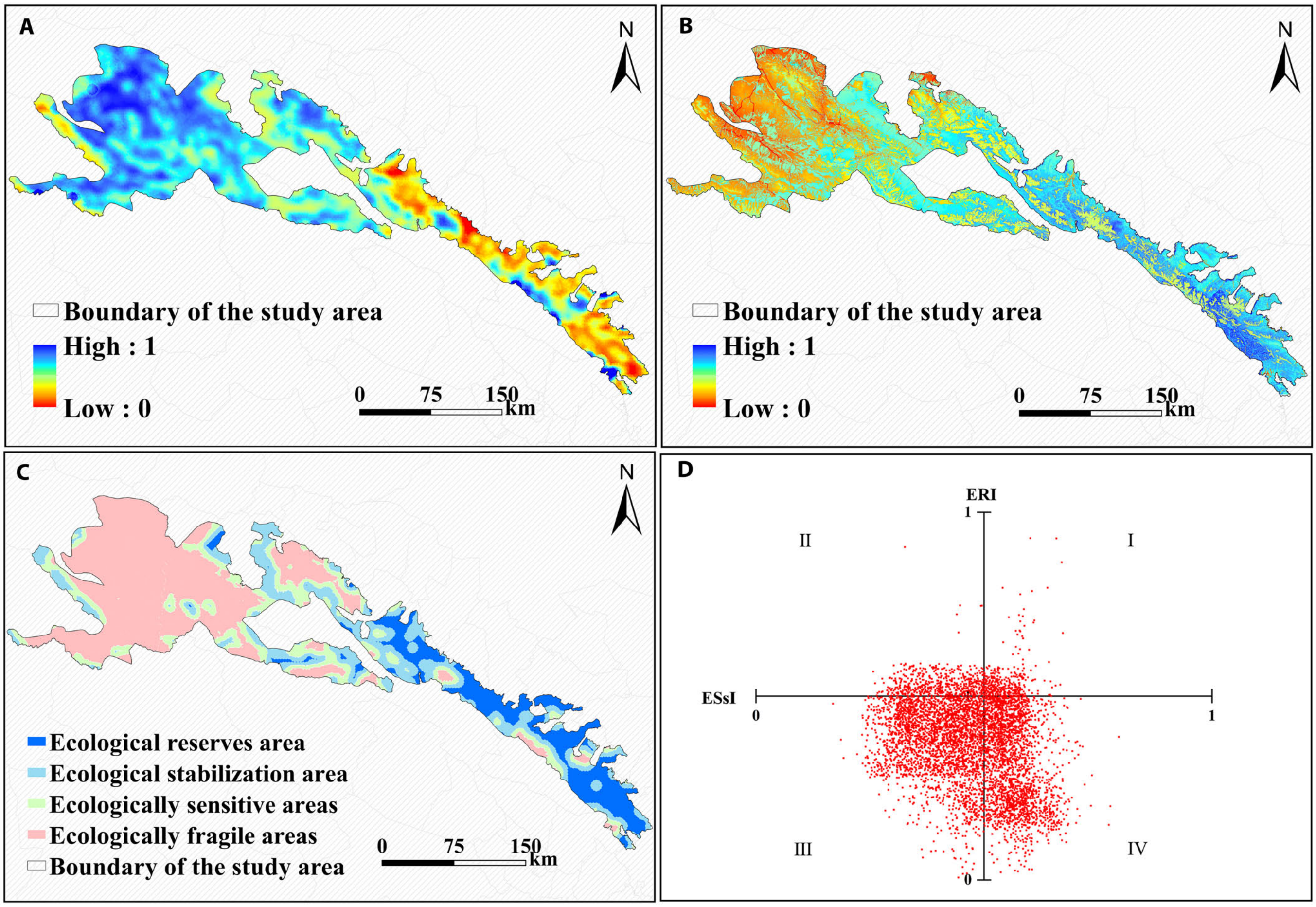

Fig. 8. Spatial distribution of ecological function zones. (A) LER index. (B) Comprehensive ES index. (C) Ecological functional zone. (D) Partition quadrant.

dual pressures of "low services and high risks"—insufficient ES provision coupled with significant ecological hazards (Fig.8C).

Driving force

Factor detector

Based on the q-statistic results derived from the Geodetector model, this study elucidates the dominant driving factors and their differential explanatory power for LER across various ecological functional areas in Qilian Mountain National Park (Supplementary Material 1, Fig. S1 and Supplementary Material 7, Table S11).

In ecologically reserves areas, the factor influence hierarchy was NPP (f) > DEM (a) > average annual temperature (e) > population density (d) > GDP (i) > average annual precipitation (h) > slope (b) > distance to road (g) > distance to water system (c). The dominant role of NPP (f) underscores its status as a key regulatory factor for ecological security, with higher values indicating greater ecosystem stability and resilience. DEM (a) emerges as a secondary determinant. Anthropogenic factors (g, c) exhibit relatively weak explanatory power. In ecologically stable areas, a distinct driving pattern emerges: Annual precipitation (h, $q = 0.338$) exerts the most significant influence; GDP (I, $q = 0.202$) is a secondary factor, while topographical factors (a, b) have a lesser impact. In ecologically sensitive areas, all factors exhibit relatively weak explanatory power ($0.002 \leq q \leq 0.123$). Annual average precipitation (h) exhibits relative importance ($q = 0.123$), while GDP (i) shows much lower importance (with a $q = 0.002$). In ecologically fragile regions, the study identified a 3-factor control system: NPP (f), annual mean temperature (e), and annual mean precipitation (h) collectively explain over 60% of risk variation. Population density exhibits lower explanatory power (d, $q = 0.002$).

Interaction detector

In ecologically fragile areas, univariate analyses indicate that the independent effects of water body distance (c) and population density (d) are weak, but their interaction exhibits a typical synergistic effect. The interaction between annual mean temperature and NPP further confirms the synergistic regulatory role of water and heat conditions on vegetation productivity (Fig. 9A).

In ecologically sensitive areas, the interaction q value between distance from roads (g) and NPP (f) increased from 0.011/0.114 during independent effects to 0.139 during interaction. Meanwhile, the interaction q values between annual precipitation (h) and all factors exceeded 0.15 (Fig. 9B).

In ecologically stable areas, this region exhibits a pronounced nonlinear enhancement effect. Although the DEM (a) has the lowest independent explanatory power ($q = 0.021$), its interaction with annual average precipitation (h) yields $q = 0.525$, while the interaction between GDP and annual average precipitation achieves $q = 0.433$. (Fig. 9C).

In ecologically reserves areas, the interaction between DEM (a) and population density (d) yielded a q value of 0.516,

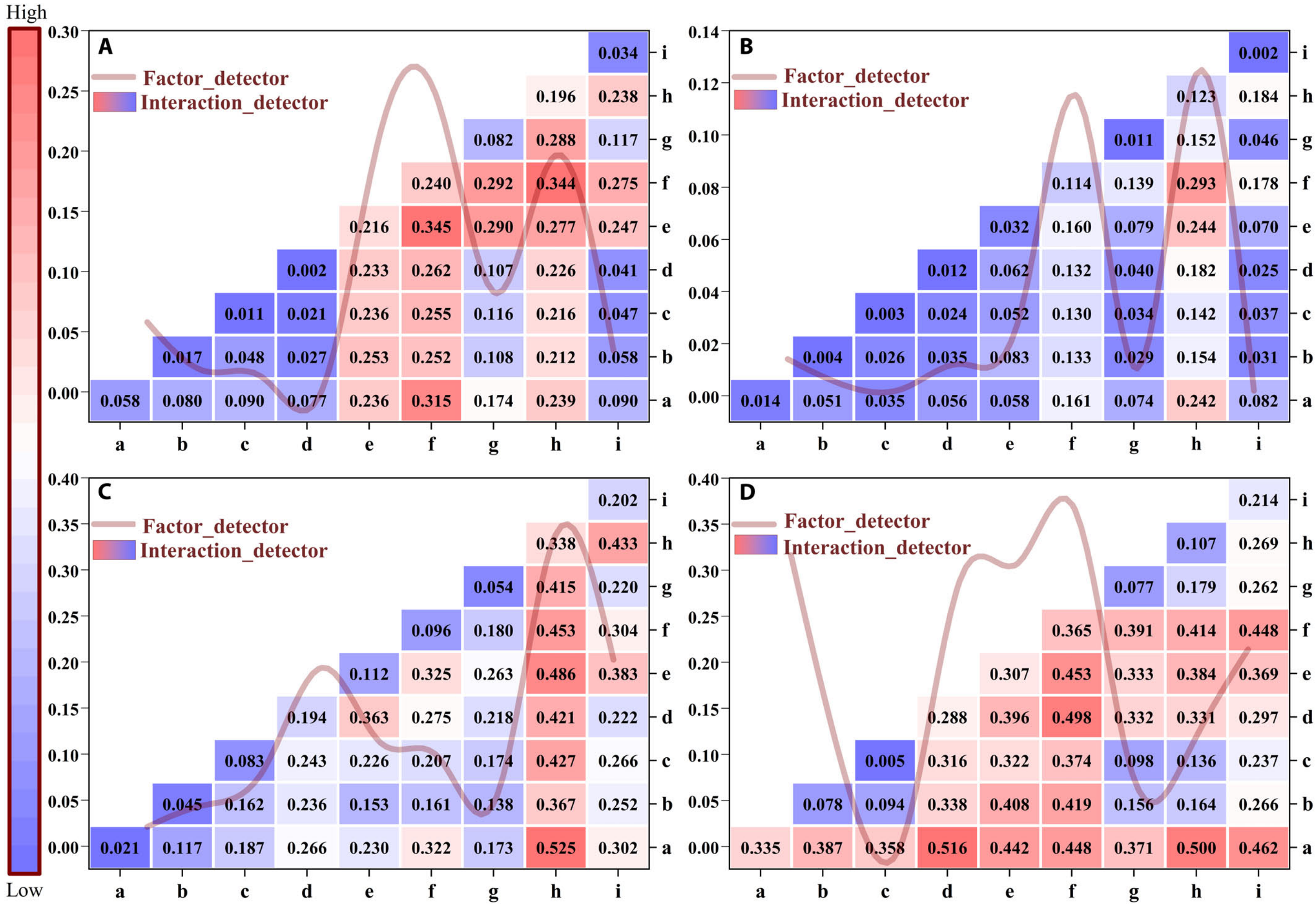

Fig. 9. Results of ecological functional zone interactions. (A) Ecologically fragile areas. (B) Ecologically sensitive areas. (C) Ecologically stable areas. (D) Ecologically reserves areas.

representing a 44% increase over its independent effect. NPP (f) exhibited significant interactions with all climatic factors ($q > 0.45$) (Fig. 9D).

Discussion

The importance of landscape pattern changes for LER

Dominant landscape types drive ecological stability with contrasting vulnerability patterns. The persistent dominance of grassland and unused land as landscape matrices, coupled with their high connectivity despite fragmentation, underscores their critical role in maintaining structural stability and ecological functions in Qilian Mountain National Park [41]. However, the pronounced fragmentation and high disturbance of construction land highlight its ecological vulnerability, suggesting that urban expansion—even in limited areas—can disproportionately impact regional risk patterns. This contrast emphasizes the need for differentiated management strategies that protect matrix-forming natural landscapes while mitigating localized anthropogenic pressures (Fig. 3) [42].

Spatiotemporal risk reduction reflects effective ecological restoration amid persistent spatial clustering. The significant decline in high-risk areas (2000–2010) and subsequent stabilization (2010–2020), consistent with the fragmentation of high-risk clusters [43], demonstrate successful restoration efforts (Fig. 4). However, the persistent west–east risk gradient and stable “high–high”/“low–low” clustering reveal inherent geospatial dependencies in ecological resilience. These findings suggest that while broad-scale restoration enhances ecosystem security, targeted interventions in western high-risk hotspots and ecotones are essential to address lingering spatial autocorrelation and fully optimize conservation outcomes (Fig. 5) [44].

The core of improving ES functions

Integrated ES improvement reflects effective conservation strategies. The consistent improvement in habitat quality, carbon sequestration, and water yield, coupled with a dramatic reduction in soil erosion, demonstrates the synergistic effectiveness of Qilian Mountain National Park’s conservation measures (Fig. 6). The spatial patterns—persistent southeast–northwest gradients in habitat quality and east–west contrasts in carbon storage—suggest that ecosystem responses are mediated by both natural environmental gradients and targeted restoration efforts, particularly in erosion-prone eastern areas. These findings highlight the importance of landscape-scale protection policies in simultaneously enhancing multiple ESs while underscoring the need for spatially adaptive management to address residual heterogeneity in service delivery [45].

Relationship between ecological risk and service response and innovation

Spatially heterogeneous risk-service relationships reveal context-dependent conservation priorities. The MGWR analysis uncovers critical spatial nonstationarity in how LER influences ESs (Fig. 7), with (a) divergent risk-service couplings—positive habitat quality–risk relationships in the southeast contrast with strongly negative carbon storage impacts in foothill regions, demonstrating that "one-size-fits-all" risk mitigation strategies are inadequate; (b) scale-dependent effectiveness of interventions—the tripling of soil retention coefficients in eastern zones verifies targeted restoration success, while persistent water yield vulnerabilities in western grasslands demand alternative approaches; (c) policy implications—the dominance of negative carbon–risk relationships underscores the urgency of prioritizing carbon-rich areas, whereas habitat quality's localized positive feedbacks suggest that some ecosystems may exhibit adaptive resilience [46]. These findings advocate for spatially intelligent management that aligns zone-specific risks with service provisioning capacities.

Notably, compared with existing studies, this research marks the first attempt to conduct ecological functional zoning by examining the response relationship between LERs and ES functions. This innovation not only further refines the overall research framework—strengthening its theoretical rigor and practical applicability—but also initially explores the framework's universality, aiming to lay the groundwork for its future promotion and application in ecological functional zoning for other national parks within China's national park network. Under the innovative framework, Qilian Mountain National Park shows southeast–northwest differences: southeast "high service–high risk" areas need urgent protection, northwest "low service–high risk" areas need restoration. This zoning-based framework guides global mountain protected areas [47].

Ecological functional zone and policies

This study established a 2-dimensional "risk-service" oriented ecological functional zone framework for the Qilian Mountain National Park, which accurately captures the inherent spatial differentiation patterns of mountain ecosystems and provides practical evidence for the park's precise ecological management. This framework centers on the core linkage of "landscape ecological risk (pressure)–ecosystem services (status)", breaking through the limitations of traditional functional zoning that relies solely on land-use or vegetation type classifications. It achieves a deep coupling between "ecological patterns–functional processes–management needs", offering a new paradigm for scientific zoning and differentiated management in mountain protected areas.

The framework reveals a "southeast–northwest dichotomy" and a "risk-service inverse spatial pattern", which essentially reflect the direct influence of the spatial heterogeneity of water and thermal resources in the Qilian Mountains on the structure and function of ecosystems, fully aligning with the core principles of mountain ecology. (a) The southeastern side is an "high-service–low-risk" ecological reserves areas, with a "structurally intact natural forest ecosystem" as its core carrier. The dominant vegetation consists of cold-temperate coniferous forests such as Picea crass folia and Juniperus przewalskii, whose formation and maintenance strictly depend on the superior water and heat conditions in the southeastern segment: Under the combined influence of the East Asian monsoon and westerly circulation, the annual precipitation in the region reaches 400 to 800 mm, and the elevation gradient precisely matches the growth threshold for coniferous forests. From an ecological functional perspective, natural forest ecosystems exhibit high biodiversity, complex community structure, and high functional redundancy: On the one hand, they efficiently provide core ecological services such as water yield, carbon storage, and habitat quality maintenance; on the other hand, they can withstand mild natural disturbances through their community self-regulation capabilities, thus exhibiting a "low-risk" characteristic. This pattern strictly follows the scientific logic that "water and heat conditions determine vegetation types, and vegetation types regulate service capacity and ecological stability". (b) The northwest side is a "low-service—high-risk" ecological fragile area (ecological fragile areas), where grasslands and unused land dominate the landscape. This is because the northwest section belongs to an arid–semiarid climate zone—annual precipitation is less than 200 mm, and evaporation exceeds 1,500 mm. The imbalance between water and heat leads to an inherently simplified ecosystem structure, with a single community layer and NPP less than one-third of that in the southeastern forest area, resulting in extremely weak disturbance resistance. From the perspective of the "service–risk" coupling relationship, the simplified ecological structure not only results in inherently insufficient service capacities such as water production and carbon sequestration but also exposes the region to extremely high ecological risks: Under drought conditions, the soil wind erosion modulus reaches 500 to 1,000 t/(km^2·a), grassland degradation rates exceed 30%, and the natural recovery period after damage can last 10 to 20 years, ultimately forming a "low service capacity and high risk overlap" pattern, which is completely consistent with the "structure–function–stability" coupling mechanism of arid zone ecosystems.

To clarify the formation mechanism of ecological risks in different functional zones, the study used Geodetector analysis to identify a "hierarchical, interactive" control system for LERs at the functional zone scale, providing a scientific basis for targeted management. Context-dependent drivers reveal complex ecological risk formation mechanisms. The Geodetector analysis uncovers a hierarchical and interactive control system governing LER across functional zones. Zone-specific dominance: While NPP and DEM drive reserves, precipitation–GDP interactions dominate stable areas, exposing how core regulators shift with ecosystem vulnerability levels. Nonlinear amplification effects enhancement of q values through factor interactions demonstrates that conventional single-factor management approaches grossly underestimate risk complexity. Climate–vegetation–human nexus: The universal enhancement of NPP–climate interactions across zones verifies vegetation's pivotal role in mitigating climate pressures, yet road–NPP antagonism in sensitive areas warns against infrastructure-driven fragmentation. These findings necessitate paradigm shifts from isolated to integrated driver management, prioritizing altitude-stratified activity regulation in reserves, precipitation–smart economic planning in stable zones, and hydrological–vegetation coupled restoration in fragile areas [48].

Finally, based on the differences in "structure–function–stability" among the 4 functional zones, the study proposed adaptive management strategies. (a) Ecologically reserves areas: Prioritize protection and maintain structural integrity: Given the characteristics of "dominated by natural forests and stable functions", no excessive intervention measures are proposed; instead, protection is used to maintain their natural state—the scientific basis lies in the fact that the "self-organizing capacity" of mature natural forest ecosystems has reached a dynamic equilibrium. Artificial interventions may instead disrupt community structure. Therefore, "conservation as a priority" is the optimal strategy to maintain their high service capacity. (b) Ecologically stabilization areas: Protective regulation and gradual restoration: Based on the "low service–low risk" characteristics, the proposal is to "gradually enhance services through targeted restoration" rather than radical changes—this aligns with the laws of ecosystem succession: The ecosystems in this region have not been severely damaged and only require mild interventions to promote positive community succession, avoiding artificial interventions that exceed the ecosystem's "carrying capacity threshold". (c) Ecologically sensitive areas: Sustainable use within carrying capacity constraints: Emphasizing that "use intensity does not exceed ecological carrying capacity", the scientific core is the "sustainable supply threshold of ecosystem services"—for example, if tourism or livestock farming is present in the area, carrying capacity should be calculated based on indicators such as "water retention capacity" and "soil carbon pool stability" to avoid overuse leading to vegetation damage, which could result in irreversible declines in service capacity. (d) Ecologically fragile areas: Emergency restoration and multi-measure coordination: Given the characteristics of "simple structure and dual pressures", a comprehensive approach combining "vegetation restoration and soil and water conservation" is proposed. The scientific basis lies in the fact that the key to ecological restoration in arid regions is "stabilizing the foundation first, then enhancing functions": Vegetation restoration increases ground cover, reducing wind and water erosion (lowering risks). Soil and water conservation measures can improve soil moisture conditions, providing support for vegetation growth (enhancing services). The 2 form a positive feedback loop of "risk reduction–service enhancement", aligning with the scientific approach of "first disaster control, then quality improvement" in arid region ecological restoration.

Limitations and future research

Data and methodological limitations: The data used in this study to quantify landscape patterns, assess ecological risks, and evaluate ESs primarily originate from existing research. The authenticity and reliability of these data are difficult to ascertain. Furthermore, the assessment of ES functions primarily relied on existing models. The obtained results could only be evaluated through subjective judgment or comparison with previous studies, and their cross-regional applicability has not been fully validated. This issue may also compromise the robustness of the findings.

Limitations in analyzing multi-factor interactions: While the study mentions the interactive effects of drivers like climate and human activities, it does not explicitly explore nonlinear relationships, lag effects, or threshold effects. This may limit the depth of analysis into complex driving mechanisms.

To solve limitations in data, method, and multi-factor analysis, future studies optimize 2 aspects: enhance data/model (field orbs, multi-source validation) and use GAMs (generalized additive models) to deepen multi-factor analysis and build "data–method" cycle, boosting eco-management guidance.

Conclusion

This study constructed a landscape risk model and employed InVEST to quantify ES functions, analyzing the risk-service response relationship within Qilian National Park. It delineated 4 functional zones and identified the driving factors for each area through geographic detectors.

1. The LER of Qilian Mountain National Park shows significant positive spatial correlation; local spatial autocorrelation reveals strong spatial interaction and similar neighborhood risk values. From 2000 to 2020, risk spatial aggregation decreased, risks declined, and landscape ecological conditions improved overall.

2. Habitat quality, carbon sequestration, and water yield in Qilian Mountain National Park improved significantly from 2000 to 2020, and soil erosion was sharply reduced, but the difference in the gradient between the southeast and the northwest highlights the dual regulatory role of natural and anthropogenic restoration.

3. The impact of ecological risk on services in Qilian Mountain Park is spatially nonstationary—habitat quality in the southeast is positively correlated with risk, while carbon sequestration is generally suppressed by risk, revealing that the vicious circle of "low function amplifies risk" needs to be broken by zones.

4. This study established a 2-dimensional "risk-service" oriented ecological zoning framework for Qilian Mountain National Park, precisely capturing the spatial variability of mountain ecosystems. Centered on the "risk-service" coupling, it integrates the dimensions of "pattern–process–service–sustainability", providing a new paradigm and empirical support for targeted management of mountain protected areas.

5. For ecologically reserves areas, prioritize conservation to maintain natural conditions and avoid excessive intervention that could disrupt community structures. For ecologically stable areas, implement targeted restoration measures to gradually enhance ESs. For ecologically sensitive areas, enforce soil and water conservation policies to prevent overuse from tourism or livestock grazing. For ecologically fragile areas, adopt emergency restoration combining vegetation rehabilitation with soil and water conservation, alongside multi-measure coordinated plans.

Acknowledgments

We would like to express our sincere gratitude to the editors and reviewers who have put considerable time and effort into their comments on this paper.

Funding: This work was supported by the Gansu Agricultural University Scientific Research Start-up Project, China (GAU-KYQD-2022-50); the Major Scientific and Technological Tasks of Gansu Province—The Central Government to Guide Local Science and Technology Development Funds (25ZYJA032); the Natural Science Foundation of Gansu Province (25JRRA358 and 24JRRA774); and the Teachers' Innovation Fund Program of Gansu Education Department (2025A-098, 2025B-096, and 2025B-110).

Author contributions: J.G.: Conceptualization, methodology, software, data collection, curation and analysis, formal analysis, and writing—original draft. N.P.: writing—review and editing. D.Z.: Supervision.

Competing interests: The authors declare that they have no competing interests.

Data Availability

All data included in this study are available upon request by contacting the corresponding author.

Supplementary Materials

Supplementary Materials 1 to 7
Figs. S1 and S2
Tables S1 to S11

References

1. Rockström J, Gupta J, Qin D, Lade SJ, Abrams JF, Andersen LS, Armstrong McKay DI, Bai X, Bala G, Bunn SE, et al. Safe and just Earth system boundaries. *Nature*. 2023;619(7968):102–111.
2. Scheffer M, Carpenter SR, Lenton TM, Bascompte J, Brock W, Dakos V, van de Koppel J, van de Leemput IA, Levin SA, van Nes EH, et al. Anticipating critical transitions. *Science*. 2012;338(6105):344–348.
3. Haddad NM, Brudvig LA, Clobert J, Davies KF, Gonzalez A, Holt RD, Lovejoy TE, Sexton JO, Austin MP, Collins CD, et al. Habitat fragmentation and its lasting impact on Earth's ecosystems. *Sci Adv*. 2015;1(2):Article e1500052.
4. Newbold T, Hudson LN, Hill SLL, Contu S, Lysenko I, Senior RA, Börger L, Bennett DJ, Choimes A, Collen B, et al. Global effects of land use on local terrestrial biodiversity. *Nature*. 2015;520:45–50.
5. Hooper DU, Adair EC, Cardinale BJ, Byrnes JEK, Hungate BA, Matulich KL, Gonzalez A, Duffy JE, Gamfeldt L, O'Connor MI. A global synthesis reveals biodiversity loss as a major driver of ecosystem change. *Nature*. 2012;486(7401):105–108.
6. Díaz S, Pascual U, Stenseke M, Martín-López B, Watson RT, Molnár Z, Hill R, Chan KMA, Baste IA, Brauman KA, et al. Assessing nature's contributions to people. *Science*. 2018;359(6373):270–272.
7. Fu B, Wu X, Wang Z, Wu X, Wang S. Coupling human and natural systems for sustainability: Experience from China's Loess Plateau. *Earth Syst Dynam*. 2022;13(2):795–808.
8. Seto KC, Güneralp B, Hutyra LR. Global forecasts of urban expansion to 2030 and direct impacts on biodiversity and carbon pools. *Proc Natl Acad Sci USA*. 2012;109(40): 16083–16088.
9. Zhang K, Fang B, Oleson K, Zhao L, He C, Huang Q, Liu Z, Cao C, Lee X. Urban land expansion amplifies surface warming more in dry climate than in wet climate: A global sensitivity study. *J Geophys Res Atmos*. 2025;130(4): Article e2024JD041696.
10. Houghton RA. Interactions between land-use change and climate-carbon cycle feedbacks. *Curr Clim Chang Rep*. 2018;4(2):115–127.
11. Wu J. Landscape sustainability science: Ecosystem services and human well-being in changing landscapes. *Landsc Ecol*. 2013;28(6):999–1023.
12. Bennett EM, Cramer W, Begossi A, Cundill G, Díaz S, Egoh BN, Geijzendorffer IR, Krug CB, Lavorel S, Lazos E, et al. Linking biodiversity, ecosystem services, and human well-being: Three challenges for designing research for sustainability. *Curr Opin Environ Sustain*. 2015;14:76–85.
13. Mitchell MGE, Suarez-Castro AF, Martinez-Harms M, Maron M, McAlpine C, Gaston KJ, Johansen K, Rhodes JR. Reframing landscape fragmentation's effects on ecosystem services. *Trends Ecol Evol*. 2015;30(4):190–198.
14. Li Q, Wei X, Zhang M, Liu W, Fan H, Zhou G, Giles-Hansen K, Liu S, Wang Y. Forest cover change and water yield in large forested watersheds: A global synthetic assessment. *Ecohydrology*. 2017;10(4):Article e1838.
15. Steffan-Dewenter I, Potts SG, Packer L. Pollinator diversity and crop pollination services are at risk. *Trends Ecol Evol*. 2005;20:651–652.
16. Bian J, Chen W, Zeng J. Ecosystem services, landscape pattern, and landscape ecological risk zoning in China. *Environ Sci Pollut Res*. 2023;30(7):17709–17722.
17. Palomo I, Locatelli B, Otero I, Colloff M, Crouzat E, Cuni-Sanchez A, Gómez-Baggethun E, González-García A, Grêt-Regamey A, Jiménez-Aceituno A, et al. Assessing nature-based solutions for transformative change. *One Earth*. 2021;4(5):730–741.
18. Kang P, Chen W, Hou Y, Li Y. Spatial-temporal risk assessment of urbanization impacts on ecosystem services based on pressure-status - response framework. *Sci Rep*. 2019;9(1):16806.
19. Peng J, Liu Y, Liu Z, Yang Y. Mapping spatial non-stationarity of human-natural factors associated with agricultural landscape multifunctionality in Beijing–Tianjin–Hebei region, China. *Agric Ecosyst Environ*. 2017;246:221–233.
20. Shouzhang P. *1-km monthly precipitation dataset for China (1901-2023)*. Beijing (China): National Tibetan Plateau Data Center; 2024.
21. Shouzhang P. *1-km monthly mean temperature dataset for china (1901-2023)*. Beijing (China): National Tibetan Plateau Data Center; 2024.
22. Shouzhang P. *1-km monthly potential evapotranspiration dataset for China (1901-2023)*. Beijing (China): National Tibetan Plateau Data Center; 2024.
23. Batjes NH. Harmonized soil property values for broad-scale modelling (WISE30sec) with estimates of global soil carbon stocks. *Geoderma*. 2016;269:61–68.
24. Frazier AE, Kedron P. Landscape metrics: Past progress and future directions. *Curr Landsc Ecol Rep*. 2017;2:63–72.
25. Hagen-Zanker A. A computational framework for generalized moving windows and its application to landscape pattern analysis. *Int J Appl Earth Obs Geoinf*. 2016;44:205–216.
26. Guo H, Cai Y, Li B, Wan H, Yang Z. An improved approach for evaluating landscape ecological risks and exploring its coupling coordination with ecosystem services. *J Environ Manag*. 2023;348:Article 119277.
27. Meraj G, Singh SK, Kanga S, Islam MN. Modeling on comparison of ecosystem services concepts, tools, methods and their ecological-economic implications: A review. *Modeling Earth Syst Environ*. 2022;8:15–34.
28. Wang S, Chen H, Su W, Cui S, Xu Y, Zhou Z. Research on habitat quality assessment and decision-making based on semi-supervised ensemble learning method—Daxia River Basin, China. *Ecol Indic*. 2023;156:Article 111153.
29. Li X, Zhu J, Lyu X, Sun Y, Tan C, Zhang B, Tarolli P, Yang Q. An integrative conservation and management strategy based on biological and cultural diversity assessment: A case study of Miaoling mountainous region, China. *Ecol Indic*. 2025;171:Article 113187.
30. Pei R, Ma B, Liu S, Su J, Yu M, Li W. Spatiotemporal differentiation and trade-offs and synergies of ecosystem services in Qilian Mountains National Park. *Ecol Indic*. 2024;169:Article 112891.
31. Gashaw T, Worqlul AW, Dile YT, Sahle M, Adem AA, Bantider A, Teixeira Z, Alamirew T, Meshesha DT, Bayable G. Evaluating InVEST model for simulating annual and seasonal water yield in data-scarce regions of the Abbay (Upper Blue Nile) Basin: Implications for water resource planners and managers. *Sustain Water Res Manage*. 2022;8:170.
32. Hamel P, Falinski K, Sharp R, Auerbach DA, Sánchez-Canales M, Dennedy-Frank PJ. Sediment delivery modeling in practice: Comparing the effects of watershed characteristics and data resolution across hydroclimatic regions. *Sci Total Environ*. 2017;580:1381–1388.

33. Yang Y, Zheng H, Kong L, Huang B, Xu W, Ouyang Z. Mapping ecosystem services bundles to detect high- and low-value ecosystem services areas for land use management. *J Clean Prod*. 2019;225:11–17.
34. Liang Y, Song W. Integrating potential ecosystem services losses into ecological risk assessment of land use changes: A case study on the Qinghai-Tibet Plateau. *J Environ Manag*. 2022;318:Article 115607.
35. Altman N, Krzywinski M. Simple linear regression. *Nat Methods*. 2015;12:999–1000.
36. Lu B, Martin C, Paul H, Fotheringham AS. Geographically weighted regression with a non-Euclidean distance metric: A case study using hedonic house price data. *Int J Geogr Inf Sci*. 2014;28(4):660–681.
37. Fotheringham AS, Wenbai Y, Kang W. Multiscale geographically weighted regression (MGWR). *Ann Am Assoc Geogr*. 2017;107(6):1247–1265.
38. Getis A. Spatial autocorrelation. In: Fischer MM, Getis A, editors. *Handbook of applied spatial analysis: Software tools, methods and applications*. Berlin, Heidelberg: Springer Berlin Heidelberg; 2010. p. 255–278.
39. Anselin L. Local indicators of spatial association—LISA. *Geogr Anal*. 1995;27(2):93–115.
40. Jinfeng W, Chengdong XU. Geodetector: Principle and prospective. *Acta Geograph Sin*. 2017;72:116–134.
41. Guo Y, Boughton EH, Bohlman S, Bernacchi C, Bohlen PJ, Boughton R, DeLucia E, Fauth JE, Gomez-Casanovas N, Jenkins DG, et al. Grassland intensification effects cascade to alter multifunctionality of wetlands within metaecosystems. *Nat Commun*. 2023;14:8267.
42. Zhang Y, Yang Z, Yang R, Liu F, He Y, Cao L, Yang J, Zhang J. Ecological risk assessment and response prediction caused by LUCC in the central Yunnan Province. *Sci Rep*. 2025;15:2416.
43. Niu X, Zhang J, Wang S, Zong L, Zhou M, Zhang M. Identification of priority areas for ecological restoration based on ecological security patterns and ecological risks: A case study of the Hefei Metropolitan Area. *Ecol Indic*. 2025;175:Article 113590.
44. Gong J, Cao E, Xie Y, Xu C, Li H, Yan L. Integrating ecosystem services and landscape ecological risk into adaptive management: Insights from a western mountain-basin area, China. *J Environ Manage*. 2021;281:Article 111817.
45. Gao C, Hu B, Wang Z, Huang S, Zhang L. Study on spatiotemporal changes of ecosystem service trade-offs/synergies and driving mechanisms in the key zone of mountain-river-sea coupling: A case study of the southwest Guangxi Karst-Beibu Gulf. *Ecol Indic*. 2024;169:Article 112892.
46. Qin H, Li S, Sun J, Cheng J. Scale-dependent responses of ecosystem service trade-offs to urbanization in Erhai Lake Basin, China. *Environ Sci Pollut Res Int*. 2023;30:120663–120682.
47. Jiang X, Wang B, Fang Q, Bai P, Guo T, Wu Q. Ecological Zoning Management Strategies in China: A Perspective of Ecosystem Services Supply and Demand. *Land*. 2024;13(7):1112.
48. Ni Z, Zhao Y, Liu J, Li Y, Xia X, Zhang Y. Navigating ecological–economic interactions: Spatiotemporal dynamics and drivers in the lower reaches of the Jinsha river. *Land*. 2024;13(12):2159.

Ecosystem Health and Sustainability
A SCIENCE PARTNER JOURNAL

Integrating Landscape Ecological Risk and Ecosystem Services for Ecological Zoning in the Qilian Mountain National Park

Juchuan Gao, Ninghui Pan, and Dongmei Zhou

Citation: Gao J, Pan N, Zhou D. Integrating Landscape Ecological Risk and Ecosystem Services for Ecological Zoning in the Qilian Mountain National Park. *Ecosyst Health Sustain*. 2025;**11**:0441. DOI: 10.34133/ehs.0441

Qilian Mountain National Park, serving as a vital ecological barrier in northwest China, urgently requires achieving a balance between conservation and management. This study aims to elucidate the spatiotemporal dynamics of landscape patterns, landscape ecological risks (LERs), and ecosystem services (ESs), and reveal their response relationships. Based on risk-service response optimization, ecological zoning is established, and adaptive strategies are proposed. The research integrates multi-source data within a “pattern–process–service–sustainability” framework, employing methods including landscape indices, the multiscale geographically weighted regression (MGWR) model, the LER-ES coupling model, and the Geodetector model. Key findings are as follows: (a) Landscape fragmentation decreased by 12.3% from 2000 to 2020, with an average annual reduction of 2.1% in LER and weakened spatial clustering intensity. An east–west gradient in LER persisted. (b) The comprehensive capacity of ESs improved, exhibiting a southeast–northwest gradient distribution. (c) The MGWR model confirmed that LER negatively impacts ecological services, with spatial nonstationarity present. (d) Ecological zones were classified into protected areas, stable areas, sensitive areas, and vulnerable areas, with obvious differences in driving factors—environmental vulnerability was primarily dominated by natural factors, while relatively stable areas were more significantly influenced by human activities. This represents the first zoning based on the risk-service relationship, breaking through traditional limitations.
Image

View the article online
https://spj.science.org/doi/10.34133/ehs.0441

Ecosystem Health and Sustainability (ISSN 2332-8878) is published by the American Association for the Advancement of Science. 1200 New York Avenue NW, Washington, DC 20005.